Research Paper

Trichloromethane dechlorination by a novel *Dehalobacter* sp. strain 8M reveals a third contrasting C and Cl isotope fractionation pattern within this genus

Jesica M. Soder-Walz [a], Clara Torrentó [b], Camelia Algora [c], Kenneth Wasmund [d], Pilar Cortés [e], Albert Soler [b], Teresa Vicent [a], Mònica Rosell [b,*], Ernest Marco-Urrea [a]

[a] *Departament d'Enginyeria Química, Biològica i Ambiental, Universitat Autònoma de Barcelona (UAB), Carrer de les Sitges s/n, Bellaterra, Spain*
[b] *Grup MAiMA, Mineralogia Aplicada, Geoquímica i Geomicrobiologia, Departament de Mineralogia, Petrologia i Geologia Aplicada, Facultat de Ciències de la Terra, Institut de Recerca de l'Aigua (IdRA), Universitat de Barcelona (UB), c/ Martí Franquès s/n, 08028 Barcelona, Spain*
[c] *Laboratory of Environmental Microbiology, Institute of Microbiology of the Czech Academy of Sciences, Vídeňská 1083, 14220, Praha 4, Czech Republic.*
[d] *Division of Microbial Ecology, Centre for Microbiology and Environmental Systems Science, University of Vienna, Vienna 1010, Austria.*
[e] *Departament de Genètica i de Microbiologia, Facultat de BioCiències, Universitat Autònoma de Barcelona, 08193, Bellaterra, Barcelona, Spain.*

HIGHLIGHTS

- Novel *Dehalobacter* strain 8M anaerobically dechlorinates TCM to DCM.
- Strain 8M shares around 99.2% 16S rRNA gene similarity with strains CF and UNSWDHB.
- Significantly different TCM dual CCl isotope fractionation pattern of strain 8M.
- Consistent $\Lambda^{C/Cl}$ in enzymatic assays points to enzyme binding as rate-limiting step.

GRAPHICAL ABSTRACT
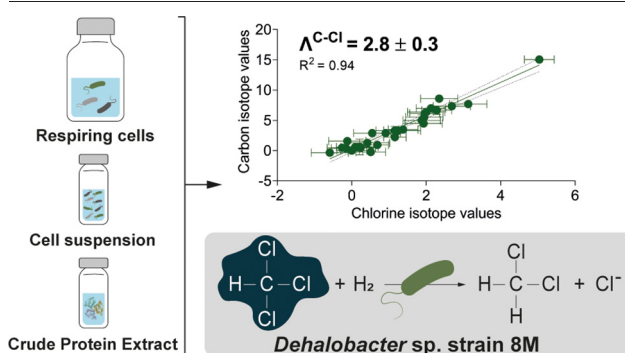
ARTICLE INFO

ABSTRACT

Trichloromethane (TCM) is a pollutant frequently detected in contaminated aquifers, and only four bacterial strains are known to respire it. Here, we obtained a novel *Dehalobacter* strain capable of transforming TCM to dichloromethane, which was denominated *Dehalobacter* sp. strain 8M. Besides TCM, strain 8M also completely transformed 1,1,2-trichloroethane to vinyl chloride and 1,2-dichloroethane. Quantitative PCR analysis for the 16S rRNA genes confirmed growth of *Dehalobacter* with TCM and 1,1,2-trichloroethane as electron acceptors. Carbon and chlorine isotope fractionation during TCM transformation was studied in cultured cells and in enzymatic assays with cell suspensions and crude protein extracts. TCM transformation in the three studied systems resulted in small but significant carbon ($\varepsilon_C = -2.7 \pm 0.1$‰ for respiring cells, -3.1 ± 0.1‰ for cell suspensions, and -4.1 ± 0.5‰ for crude protein extracts) and chlorine ($\varepsilon_{Cl} = -0.9 \pm 0.1$‰, -1.1 ± 0.1‰, and -1.2 ± 0.2‰, respectively) isotope fractionation. A characteristic and consistent dual CCl isotope fractionation pattern was observed for the three systems (combined $\Lambda^{C/Cl} = 2.8 \pm 0.3$). This $\Lambda^{C/Cl}$ differed significantly from previously reported values for anaerobic dechlorination of TCM by the corrinoid cofactor vitamin B12 and other *Dehalobacter* strains. These findings widen our knowledge on the existence of different enzyme binding mechanisms underlying TCM-dechlorination within the genus *Dehalobacter* and demonstrates that dual isotope analysis could be a feasible tool to differentiate TCM degraders at field studies.

* Corresponding author at: Grup MAiMA, SGR Mineralogia Aplicada, Geoquímica i Geomicrobiologia, Departament de Mineralogia, Petrologia i Geologia Aplicada, Facultat de Ciències de la Terra, Institut de Recerca de l'Aigua (IdRA), Universitat de Barcelona (UB), c/ Martí Franquès s/n, 08028 Barcelona, Spain.
E-mail address: monica.rosell@ub.edu (M. Rosell).

1. Introduction

Trichloromethane (TCM), commonly known as chloroform ($CHCl_3$), has been extensively used in industrial applications as a solvent, cleaning agent, and precursor in the production of pesticides and fire extinguishing agents, among others. When released to soil, mostly from accidental spills or leaking storage tanks in chemical manufacturing facilities, TCM can readily accumulate at the bottom of aquifers forming a dense non-aqueous phase liquid, where it remains relatively recalcitrant to degradation and decomposition (half-life by non-alkaline hydrolysis >1000 years) (McCulloch, 2003).

Importantly, the US-EPA considers TCM as a probable human carcinogen (Agency, 2000), and prominently, TCM ranks 11th on the 2019 Agency for Toxic Substances and Disease Registry Priority List of Hazardous Substances based on a combination of its frequency, toxicity, and potential for human exposure (Substance Priority List | ATSDR, n.d.). It is also ranked 32nd on the list of priority substances in the framework of water policy of the European Union (Directive 2013/39/EU). In addition to the adverse effects on human health, TCM is a strong inhibitor of many microbial processes, including methanogenesis and organohalide respiration (Bagley et al., 2000). Therefore, when a contaminated site contains a mixture of organochlorines including TCM, its removal is a crucial first step to proceed further with the bioremediation of the accompanying chlorinated compounds. This removal of TCM can be microbially mediated in oxic and anoxic environments. A variety of primary substrates (e.g., methane, propane, butane, hexane, and toluene) can support aerobic cometabolism of TCM (Cappelletti et al., 2012). However, the prevalence of anoxic conditions in contaminated aquifers limits the in situ application of aerobic bioremediation strategies. In anoxic environments, three main biodegradation pathways have been reported for TCM: i) cometabolic reductive dechlorination, ii) hydrolysis followed by oxidation to CO_2, and iii) organohalide respiration (Cappelletti et al., 2012). Natural attenuation, biostimulation and bioaugmentation of organohalide-respiring bacteria (OHRB) are considered cost-effective and efficient approaches to transform TCM in contaminated sites (Jugder et al., 2016). To date, members of the genera *Dehalobacter* (strains CF, UNSWDHB and THM1), and *Desulfitobacterium* (strain PR) have been described as the only OHRB capable of respiring TCM, both producing DCM as the predominant transformation product (Ding et al., 2014; Grostern et al., 2010; Justicia-Leon et al., 2012; Lee et al., 2012).

A major challenge facing field-scale practitioners of bioremediation is the provision of definitive proof that biotransformation is occurring, which is often difficult to accomplish based on assessments of concentrations of chemicals alone. Compound-specific isotope analysis (CSIA) is a robust technique that can provide direct evidence and quantification of in situ biodegradation of contaminants (Kuntze et al., 2020; Nijenhuis et al., 2018; Vogt et al., 2020). The principle of CSIA is tied to measuring the underlying kinetic isotope effect (KIE) occurring during a transformation process whereby, in most cases, chemical bonds containing light isotopes (e.g., ^{12}C, ^{35}Cl) are preferentially cleaved compared with those containing one or more heavy isotopes (e.g., ^{13}C, ^{37}Cl) and, consequently, a relative enrichment of the remaining contaminant mass in molecules containing the heavier isotopes is expected (Elsner et al., 2005). These compound specific isotope effects can be evaluated according to a simplified version of the Rayleigh equation Eq. (1):

$$\ln \left(\frac{R_t}{R_0} \right) = \varepsilon \cdot \ln (f) \tag{1}$$

where ε is the isotopic fractionation (expressed on a per mill scale, ‰), f is the fraction of the remaining substrate at any given time t and R_t and R_0 are the abundance ratios of specific stable isotopes (e.g., $^{13}C/^{12}C$, $^{37}Cl/^{35}Cl$) at any time (t) and at the beginning of the reaction, respectively. The C and Cl isotopic compositions are reported as the deviation from the corresponding international reference material using the conventional $\delta^h E$ notation, where $\delta^h E = (R_{sample}/R_{standard}) - 1$, E is the considered element (C and

Cl), and h is the atomic mass of the heavy isotope (13 for C and 37 for Cl). Since variations in isotope ratios are often small, the $\delta^h E$ values are expressed on a per mill scale (‰).

The theoretical background and the mechanistic implications of apparent isotope effects (AKIEs, the observed or measured isotope effects) in biological reactions for characterizing biotransformation of organohalides have been recently reviewed (Ojeda et al., 2020; Nijenhuis et al., 2016). In contrast to chemical homogeneous reactions where the bond cleavage provides the full expression of the KIE in many cases, in complex enzymatic systems the AKIE can be affected by rate limitation reaction steps other than bond cleavage (such as the ones related to uptake into the cell, transport within the cell or binding to the enzyme) leading to masking of isotope effects. Multi-element CSIA, which measures two or more element isotopic compositions, is expected to improve differentiation of transformation mechanisms (Ojeda et al., 2020; Nijenhuis and Richnow, 2016). Dual element isotope slopes (Λ), which correlate isotope values of two elements relative to each other, provide a sensitive parameter to differentiate reaction mechanisms while suppressing potential masking of intrinsic isotope effects affecting in a similar degree each element of the molecule (Ojeda et al., 2020). However, some exceptions have been already found for different enzymes catalyzing the same exact reaction likely via different transition states or connected to enzyme-substrate binding (Rosell et al., 2012; Renpenning et al., 2014; Gafni et al., 2020). Therefore, an indirect assessment of these isotope-masking effects can be performed by using cell suspensions (concentrate of active intact cells) and/or crude protein extracts experiments, where the cell membrane is disrupted, mass transfer is absent, and, therefore, the enzyme is directly available for electron transfer and reductive dehalogenation reactions, for instance. To date, multi-element isotope fractionation associated with TCM degradation has been reported for different biotic and abiotic reaction mechanisms as summarized by Ojeda et al. (2020), and this approach has already been used for identifying and characterizing TCM degradation at contaminated sites (Blázquez-Pallí et al., 2019; Rodríguez-Fernández et al., 2018a). With regards to the respiration of TCM, a recent study showed that two closely related *Dehalobacter* sp. (strains CF and UNSWDHB) transform TCM to DCM with unexpected opposing dual element isotope slopes (Heckel et al., 2019). Strain CF, which dechlorinates TCM by the reductive dehalogenase CfrA, exhibited identical isotope effects to those measured with the corrinoid cofactor vitamin B_{12} (dual CCl slope, $\Lambda^{C/Cl} = 6.6 \pm 0.1$ and $\Lambda^{C/Cl} = 6.5 \pm 0.2$, respectively), indicating that they likely share the same reaction mechanism, either outer-sphere-single-electron transfer (OS-SET) (Heckel et al., 2017) or S_N2 nucleophilic substitution mechanism (Heckel et al., 2019). In contrast to strain CF, strain UNSWDHB, which uses the TCM reductive dehalogenase TmrA, exhibited an unprecedented inverse chlorine isotope effects leading to an opposing dual element isotope slope ($\Lambda^{C/Cl} = -1.20 \pm 0.2$) (Heckel et al., 2019). Cell suspension and crude protein extract experiments with strain UNSWDHB were both unable to unmask the intrinsic KIE of TmrA, suggesting that enzyme binding and/or mass-transfer into the periplasm rather than mass transfer across the cell membrane were rate-limiting. This inconsistency between C and Cl isotope effects within strains belonging to the same genus opens the question about the different enzymatic reaction mechanisms underlying organohalide respiration of TCM. Values of $\Lambda^{C/Cl}$ are not reported yet for *Dehalobacter* sp. strain THM1 and *Desulfitobacterium* sp. strain PR.

To provide insight into potential isotope-masking effects and the reaction mechanisms of TCM degradation within the genus *Dehalobacter*, the goal of this work was to assess C and Cl isotope fractionation during anaerobic dechlorination of TCM by a novel *Dehalobacter* strain capable of transforming TCM to DCM. The culture was recently obtained from groundwater and fine sediments collected from a TCM-contaminated site (named "site 1" in (Blázquez-Pallí et al., 2019)). We enriched the *Dehalobacter*-containing culture responsible for TCM degradation and characterized alternative organohalogens as electron acceptors that this enrichment used. Carbon and chlorine isotope fractionation during TCM dechlorination was analyzed within distinct complexity systems levels: respiring cells growing in the culture medium during TCM respiration versus enzymatic

assays using cell suspensions and crude protein extracts (i.e., crude protein extract from lysed cells), in order to assess isotope-masking effects prior to the enzymatic reaction.

2. Experimental procedures

2.1. Chemicals, inoculum source and culture medium

All chemicals used were of the highest available purity and were listed in SMM1.

The parent enrichment culture originated from groundwater and sediments from a TCM-contaminated aquifer as previously described (Blázquez-Pallí et al., 2019). This culture was maintained in 100 mL glass serum bottles with 65 mL of an anoxic defined buffered medium (pH = 7) containing 5 mM sodium acetate, 200 mg L^{-1} yeast extract, 22.8 μM tungsten, 24.2 μM selenium, 200 μM Na$_2$S × 9H$_2$O and 200 μM L-cysteine as reducing agent, 10 mM bicarbonate as a buffer, 0.25 mg L^{-1} resazurin as a redox indicator, vitamins and trace elements as described previously (Tschech and Pfennig, 1984). The serum bottles were sealed with Teflon-coated butyl rubber stoppers and aluminum crimp caps. Halogenated compounds were added through the septum as electron acceptors and H$_2$ was gassed to 0.4 bar overpressure, supplied as an available electron donor. All experimental bottles were incubated in the dark at 25 °C. Active cultures were transferred into fresh medium (4.3% v/v inoculum) during the exponential degradation phase of the corresponding organohalogen. Abiotic controls with the above described medium and with halogenated compounds but without inoculum, were always included in triplicates to evaluate abiotic processes. The dilution-to-extinction procedure in liquid and semisolid medium was performed in an attempt to isolate the bacteria responsible for TCM transformation and the method followed is described in the Supporting Information (SMM2). Briefly, six consecutive serial dilution series in liquid medium were performed, recovering TCM dechlorinating activity within the 10^{-8} dilution tube aiming at a highest enrichment of TCM-dechlorinating bacteria. A terminal positive tube in the 10^{-8} dilution was used in the dilution-to-extinction approach with agar shakes aiming at the isolation of single colonies (see Fig. S1 in Supplementary Information).

2.2. Stable carbon and chlorine isotope experiments

Three set of experiments were performed for assessing carbon and chlorine isotope fractionation during TCM transformation using: (i) respiring cells, (ii) cell suspensions, and (iii) crude protein extracts. The preparation of cell suspensions and crude protein extracts is described in the Supporting Information (SMM3). For respiring cells, 12 parallel experimental bottles with the buffered medium were inoculated as described above and fed with 500 μM TCM. Each bottle was killed at different extents of TCM degradation by adding H$_2$SO$_4$ (final concentration in the bottle: 20 mM H$_2$SO$_4$). The samples were stored at 4 °C until further analysis. For cell suspension and crude protein extract experiments, 12 batch experiments were performed in 20 mL vials, with 10 mL of a buffered mix solution containing potassium acetate/acetic acid (K-AC) pH 7.0, 2 mM Ti (III) citrate as a reducing agent and 2 mM methyl viologen as an artificial electron donor. One mL of cell concentrate and 300 μL of protein extract were used for cell suspension and crude protein extract experiments, respectively, and fed with 300 μM TCM. The experimental vials were incubated at 25 °C in darkness, agitated at 150 rpm and killed at different times using H$_2$SO$_4$ (final concentration in the vial: 100 mM H$_2$SO$_4$). In all three scenarios, two different type of controls were included in triplicate: (i) abiotic controls containing the sterile buffered medium or buffered mix solution with TCM and without inoculum, cell concentrate or crude protein extract. This is to control potential abiotic transformations, volatile losses, or impurities from the stock solution. (ii) Biotic controls consisting of sterile buffered medium or buffered mix solution plus inoculum, cell concentrate or crude protein extract and without TCM, to evaluate the potential transfer of TCM and DCM from the inoculum sources to the experimental bottles and to correct,

if needed, the isotopic values of these potentially transferred compounds. Both controls were killed at initial and final time points of the experiment.

2.3. Analytical methods

Volatile halogenated compounds were quantified by injecting 0.5 mL headspace samples into an Agilent 6890 N gas chromatograph (GC), equipped with a DB-624 column (30 m, 0.32 mm with 0.25 mm film thickness) and a flame ionization detector, following the method of Trueba-Santiso et al. (Trueba-Santiso et al., 2017). Peak areas were calculated using Chromeleon 6.8 Chromatography Software (Dionex Corporation). Results are presented as nominal concentrations expressed in μM and the analytical uncertainty was <5%. For carbon and chlorine isotope analysis of DCM and TCM, liquid aliquots of the sacrificed experimental bottles were taken and diluted as needed in ultrapure water into 20 mL vials filled to 10 mL final volume to adjust the concentration of the pollutants for subsequent isotope signature determination. Carbon isotope analyses were performed by headspace solid phase microextraction (HS-SPME) coupled to gas chromatography isotope ratio mass spectrometry (GC-IRMS), as explained elsewhere (Blázquez-Pallí et al., 2019) and detailed in the Supplementary Information (SMM4). Samples were analyzed in duplicate and correction by daily values of calibrated in-house TCM and DCM standards was used. Chlorine isotope analyses of TCM were performed by headspace extraction coupled to gas chromatography quadrupole mass spectrometry (GC-qMS), as explained elsewhere (Torrentó et al., 2017) and detailed in the Supplementary Information (SMM4). Ten injections of each sample were performed and the two-point calibration approach was used by interspersing along the sequence two external working standards, also injected ten times each. The analytical uncertainty 1σ was ± 0.7‰ for carbon and ± 0.5‰ for chlorine isotope values.

2.4. Evaluation of isotope data

Carbon and chlorine isotopic fractionations (ε_C and ε_{Cl}) of TCM dechlorination were calculated according to the Rayleigh equation (Eq. 1) using the double logarithmic Rayleigh plot. The uncertainty for ε values was determined from the 95% confidence interval (95% CI) of the linear regression in the Rayleigh plots. The carbon isotopic mass balance ($\delta^{13}C_{SUM}$) was obtained according to Eq. (2), where X is the molar fraction of each compound relative to the total molar mass of chloromethanes assuming complete TCM reductive dehalogenation to DCM (Hunkeler et al., 1999; Aeppli et al., 2010). The uncertainty of $\delta^{13}C_{SUM}$ values was estimated by error propagation. This carbon isotopic mass balance can be used to determine if DCM is the only degradation product or if it was further degraded. Isotopic mass balance was not calculated for chlorine since DCM chlorine isotope ratios were not measured.

$$\delta^{13}C_{SUM}(‰) = X_{TCM} \cdot \delta^{13}C_{TCM} + X_{DCM}.\delta^{13}C_{DCM} \qquad (2)$$

Apparent kinetic isotope effects (AKIE), which characterize the isotope effect of the atoms at the reactive position of a molecule, were calculated following Eq. (3), where n is the total number of the atoms of the considered element (E) in the target molecule, x is the number of atoms located at the reactive site, and z the number of atoms in intramolecular isotopic competition. For TCM AKIE$_C$, $n = x = z = 1$ and for AKIE$_{Cl}$, $n = x = z = 3$. The uncertainty of AKIE values was estimated by error propagation.

$$AKIE_E = \frac{1}{1 + \left(\frac{n \cdot z}{x} \bullet \varepsilon\right)} \qquad (3)$$

Dual isotope slopes ($\Lambda^{C/Cl}$) were calculated by ordinary linear regression (OLR) of measured $\delta^{13}C$ and $\delta^{37}Cl$ data in 2D-isotope plots (i.e., $\Lambda^{C/Cl} = \Delta\delta^{13}C/\Delta\delta^{37}Cl$). The uncertainty of $\Delta\delta$ values was estimated by error propagation. The uncertainty of Λ was reported as the 95% CI. A comparison between Λ values and their uncertainties obtained in this study with the OLR and the York (Ojeda et al., 2020; Ojeda et al., 2019) regression methods is

shown in the SI. Since no systematic bias introduced by OLR was observed and because there has not been sufficient time for the York methods to be routinely adopted in 2D-CSIA studies, we therefore decided to use OLR, but show York results in the SI.

2.5. DNA extraction, 16S rRNA gene amplicon sequencing,phylogenetic analyses of 16S rRNA gene and real-time PCR (qPCR)

Details regarding cell harvesting, DNA extraction, 16S rRNA gene amplicon sequencing, phylogenetic analyses of 16S rRNA gene and real-time PCR (qPCR) are provided in the Supporting Information (SMM5).

2.6. Statistics analysis

All measured data are presented as mean ± SD of duplicate measurements for isotopic analysis and real-time PCR (qPCR); and triplicate measurements for time-course experiments. Significant differences between the dual isotope slopes for the three groups of experiments: respiring cells, cell suspensions, and crude protein extracts, were determined using unpaired Z score-test. Comparisons were made using GraphPad Prism version 8.0.2 software (GraphPad Software). Results were considered statistically significant if $p < 0.05$.

3. Results

3.1. Enrichment of TCM-degrading bacteria

After the dilution-to-extinction in liquid and consecutively in semisolid agar shakes, two different morphology of colonies appeared in the 10^{-9} and 10^{-10} dilution tubes (Fig. S1): type 1 appeared as white, small, round, and compact colonies with defined edge, and type 2 appeared as white colonies, bigger than type 1, with non-defined edge and a cotton appearance. We picked four colonies of type 1, and six colonies of type 2, and they were re-inoculated back in ten individual serum bottles spiked with 500 μM TCM in defined liquid medium. After 28 d, four out of the ten cultures exhibited degradation of TCM, one from morphological type 1 and three of morphological type 2. We then selected one active culture for each type and performed four consecutive dilution to extinction series (Fig. S1) with liquid medium that contained 500 μM TCM. After the last serial dilution, cultures were established in serum bottles with defined liquid medium and after three further transfers and stable dechlorination rates,

DNA isolation and 16S rRNA gene amplicon sequencing analysis of these cultures was performed. This showed that experimental bottles inoculated with colony type 2 were more enriched in *Dehalobacter* (20%) and contained fewer other taxa (Fig. S2). This culture line was thus selected for the following studies. This enrichment culture dechlorinated TCM after a lag phase of about five days and stoichiometric amounts of DCM were produced (Fig. S3). The repeated addition of TCM led to faster dechlorination rates without an apparent lag phase (Fig. S3), suggesting that TCM degradation was supporting growth of the dechlorinating bacteria.

In order to assess the ability of this culture to ferment DCM, several experimental bottles were established with amendments of DCM (50 μM) after removing H_2, which is known to inhibit DCM fermentation at high partial pressure (Chen et al., 2017). DCM stalled in the bottles after 120 d of incubation, indicating that this culture was not able to ferment DCM (data not shown).

3.2. Microbial community analysis and Dehalobacter phylogeny

Amplicon sequencing of 16S rRNA genes from the stable enrichment cultures derived from type 2 colonies revealed a microbial consortium composed of bacterial members belonging to the genera *Dehalobacter* (20%; phylum *Firmicutes*), *Desulfovibrio* (20%; phylum *Desulfobacterota*, formerly known as class *Deltaproteobacteria* (Waite et al., 2020; Chen et al., 2017), and *Proteiniphilum* (57%; phylum *Bacteroidetes*). The 16S rRNA gene sequence of the *Dehalobacter* contained in this enrichment was 99.66% similar to the 16S rRNA gene of *Dehalobacter restrictus* strain PERK23, indicating that the strain in our culture was likely the species *D. restrictus*. The close similarity with *D. restrictus* was further supported by phylogenetical analysis using publicly available 16S rRNA gene sequences of *Dehalobacter* and *Desulfitobacterium* strains (Fig. 1). We tentatively denominated this strain 'Dehalobacter sp. strain 8M' to simplify naming purposes in this study.

3.3. Dehalogenation of alternative electron acceptors

The capability of the *Dehalobacter* sp. strain 8M-containing culture to transform alternative halogenated compounds was assessed replacing TCM with different chloroalkanes [1,1,2-trichloroethane (1,1,2-TCA, 200 μM), 1,1,1-trichloroethane (1,1,1-TCA, 50 μM) and 1,1-dichloroethane (1,1-DCA, 50 μM)]; chloroalkenes [trichloroethylene (TCE, 100 μM) and tetrachloroethylene (PCE, 100 μM)]; chlorobenzenes [chlorobenzene
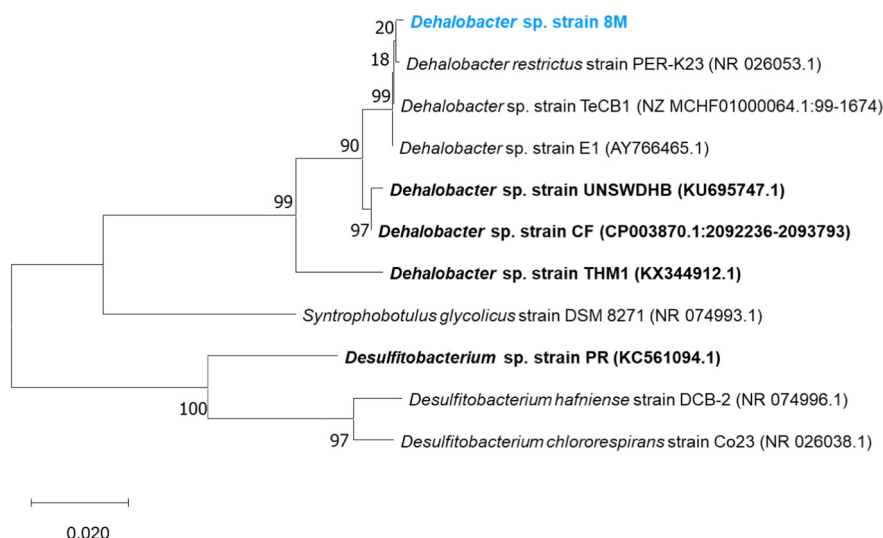

Fig. 1. Phylogenetic tree of 16S rRNA genes of *Dehalobacter* sp. strain 8M (blue) along with other strains of *Dehalobacter* and *Desulfitobacterium*. Strains known for respiring TCM are marked in bold. Phylogenetic analysis was performed using the Maximum Likelihood method and the Jukes-Cantor model. Numbers adjacent to tree branches represent percentage of branch support based on 1000 bootstrap repetitions. The scale bar shows an evolutionary distance 0.02 nucleotide substitutions per site. GenBank accession numbers are shown in parenthesis. (For interpretation of the references to colour in this figure legend, the reader is referred to the web version of this article.)

(MCB, 100 μM) and 1,2,4-trichlorobenzene (1,2,4-TCB, 100 μM)]; and the brominated analogue tribromomethane (TBM, 50 μM) in triplicate cultures.

Complete biodegradation of 1,1,2-TCA was observed after 10 days of incubation (Fig. S4), producing vinyl chloride (VC) and 1,2-dicloroethane (1,2-DCA) as degradation products in a ratio of 1:2.3, respectively. Both products accumulated in the culture medium stoichiometrically with no further biodegradation. In an attempt to determine if this *Dehalobacter* strain exhibited a preference for either TCM or 1,1,2-TCA, both compounds were added simultaneously in a culture that was grown previously with TCM. Both compounds were concomitantly dechlorinated within 10 days. However, after a second amendment, TCM was dechlorinated without an observed lag phase and 1,1,2-TCA dechlorination started after a lag phase of two days (Fig. S5).

The dechlorination of 1,1,1-TCA, 1,1-DCA and TBM was incomplete with the removal of ~22%, ~13% and ~ 48% of their starting concentrations after 130 days of incubation and produced non-stoichiometric amounts of 1,1-DCA, chloroethane (CA) and dibromomethane (DBM), respectively. These metabolites were not detected in the abiotic controls (Fig. S6).

Apart from that, no transformation of PCE, TCE, MCB and 1,2,4-TCB was observed after 130 days (data not shown).

3.4. Growth of Dehalobacter with TCM and 1,1,2-TCA

To demonstrate that *Dehalobacter* sp. strain 8M grew with TCM and 1,1,2-TCA as energy source, real-time PCR (qPCR) was performed for both cultures growing separately with TCM and 1,1,2-TCA as electron acceptors and using H_2 as the electron donor. Non-substrate controls, consisting of *Dehalobacter*-containing culture without the corresponding halogenated compound, were also analyzed at the beginning and at the end of the experiment.

When cultivated with TCM, *Dehalobacter* increased two orders of magnitude to $1.34 \cdot 10^7 \pm 2.19 \cdot 10^6$ gene copies mL^{-1} after consuming 1302 ± 54 μM TCM (Fig. 2), which corresponded to a growth yield of $2.06 \cdot 10^6 \pm 3.36 \cdot 10^5$ cells per μmol of TCM consumed (assuming 5 16S rRNA gene per genome (Kruse et al., 2013)). Similarly, *Dehalobacter* increased two orders of magnitude to $6.22 \cdot 10^7 \pm 1.00 \cdot 10^6$ gene copies mL^{-1} after consuming 1444 ± 2 μM 1,1,2-TCA, with a growth yield of $8.61 \cdot 10^6 \pm 1.39 \cdot 10^5$ cells per μmol of 1,1,2-TCA consumed. In both cultures, the growth of *Dehalobacter* in the non-substrate controls was negligible and the accumulation of the transformation products was stoichiometric with the amount of electron acceptor consumed (Fig. 2).
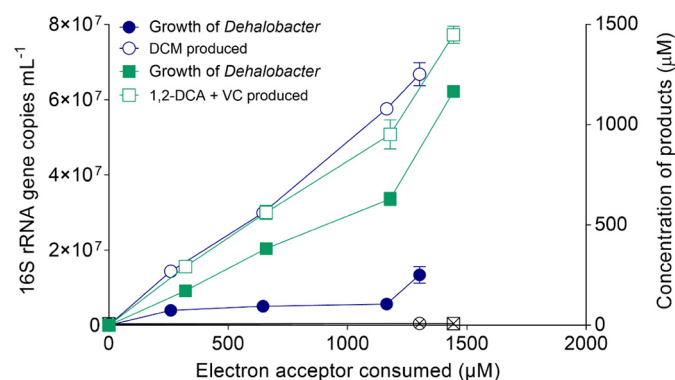

Fig. 2. Growth of *Dehalobacter* sp. strain 8M during the reductive dehalogenation of TCM (blue) and 1,1,2-TCA (green) and the concomitant accumulation of the transformation products. Error bars indicate standard deviations for triplicate bottles. Black circle and black square with an X represent the non-substrate control for TCM and 1,1,2-TCA culture respectively. (For interpretation of the references to colour in this figure legend, the reader is referred to the web version of this article.)

3.5. C and Cl isotope fractionation during TCM transformation by respiring cells, cell suspensions and crude protein extracts

In order to explore the feasibility of 2D-CSIA for assessing TCM degradation by *Dehalobacter* sp. strain 8M and provide insight into the reaction mechanism and potential isotope-masking effects within this bacterial genus, carbon and chlorine stable isotopes were measured during TCM dechlorination.

First, reductive dechlorination experiments with cultured cells of this consortium amended with 500 μM TCM were conducted ("respiring cells experiments"). The sterile abiotic controls showed no TCM degradation and the isotopic composition of TCM remained unchanged over the duration of the experiment (total average values of $\delta^{13}C = -47.8 \pm 0.1‰$ and $\delta^{37}Cl = -5.8 \pm 0.1‰$, $n = 3$). In contrast, TCM transformation up to 91% was reached in the respiring cells experiments after 9 d, with a stoichiometric release of DCM. The remaining TCM became significantly enriched in both ^{13}C (up to $-41.7 \pm 0.7‰$, Fig. S7) and ^{35}Cl isotopes (up to $-3.7 \pm 0.3‰$). The C and Cl isotopic fractionation associated with anaerobic TCM degradation by this strain was determined by the Rayleigh approach as $\varepsilon_C = -2.8 \pm 0.2‰$ ($R^2 = 0.97$) and $\varepsilon_{Cl} = -0.9 \pm 0.2‰$ ($R^2 = 0.94$), respectively (Fig. 3A and B). The $\delta^{13}C$ of the produced DCM was initially depleted in ^{13}C, in agreement with the normal isotope effect for TCM transformation, and shifted toward more ^{13}C-enriched values during the course of reaction (Fig. S7). The carbon isotopic mass balance ($\delta^{13}C_{sum} = -48.1 \pm 0.3‰$ at the end of the experiment) is consistent with the initial TCM carbon composition ($-48.3 \pm 0.1‰$, horizontal dashed line in Fig. S7). This also supports that all TCM was transformed to DCM, that no other intermediates metabolites were produced, and that DCM was not further degraded. The 2D-isotope plot ($\Delta\delta^{37}Cl$ vs. $\Delta\delta^{13}C$) showed a good fit to linear regression ($R^2 = 0.95$). A slope of $\Lambda^{C/Cl} = 2.8 \pm 0.5$ was obtained (Fig. 3C).

In order to assess potential isotope-masking effects of rate-limiting steps involving TCM diffusive transport, the system was simplified at two different complexity levels by using cell suspension (concentrate of active intact cells) and crude protein extracts (from lysed cells). Under both scenarios, TCM was transformed (up to 98% consumption) and DCM was concomitantly produced, whereas the control experiments showed no TCM degradation and a constant carbon (total average values of $-47.8 \pm 0.2‰$ for cell suspensions and $-49.1 \pm 0.5‰$ for crude protein extracts, $n = 4$) and chlorine ($-6.3 \pm 0.3‰$ and $-5.2 \pm 0.6‰$, respectively, $n = 3$) isotope composition of TCM. Significant carbon and chlorine isotopic fractionation was observed for TCM dechlorination by cell suspensions ($\varepsilon_C = -3.1 \pm 0.3‰$; $\varepsilon_{Cl} = -1.1 \pm 0.2‰$) and crude protein extract ($\varepsilon_C = -4.1 \pm 0.5‰$; $\varepsilon_{Cl} = -1.2 \pm 0.2‰$) (Fig. 3A and B). The ε_C values were statistically different ($p < 0.01$) among the three systems studied and, as expected and discussed earlier, the greatest carbon isotope effect was observed in the system with the lowest 'complexity' and therefore less masked (from $\varepsilon_C = -4.1 \pm 0.5‰$ with crude protein extracts to $-3.1 \pm 0.2‰$ with cell suspensions and $-2.8 \pm 0.2‰$ with respiring cells). The differences in ε_{Cl} values were, however, not statistically significant among the three systems ($p > 0.05$), although the trend was the same as in carbon (from $-1.2 \pm 0.2‰$ to $-1.1 \pm 0.2‰$ and $-0.9 \pm 0.2‰$, respectively).

The carbon and chlorine apparent kinetic isotope effect (AKIE$_C$ and AKIE$_{Cl}$) values obtained for the three systems are listed in Table S1 and ranged in both cases between 1.003 and 1.004. These values are much lower than the theoretical Streitwieser limit for carbon (1.057) and chlorine (1.013) KIE for CCl bond cleavage, and still lower than the suggested as realistic value with transition states at about 50% bond cleavage (KIE$_C = 1.029$ and KIE$_{Cl} = 1.007$) (Elsner et al., 2005). Therefore, the enzymatic assays (cell suspensions and crude protein extracts) were both unable to unmask the intrinsic KIE of TCM dechlorination by *Dehalobacter* sp. strain 8M discarding that TCM transport through the outer membrane neither interactions with cellular structures within the periplasmic space are important rate-limiting steps.
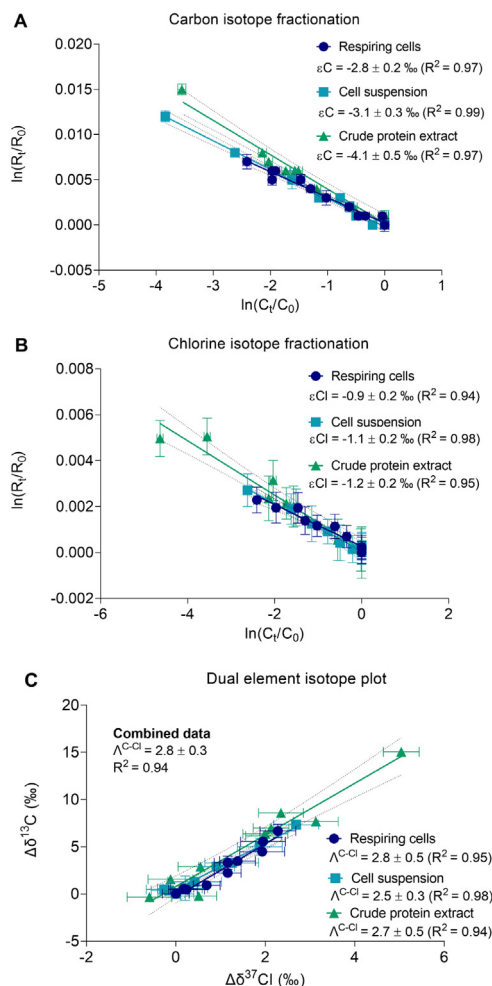
Fig. 3. Double logarithmic Rayleigh plot for carbon (A) and chlorine (B) isotope data and dual carbon and chlorine isotope plot (C) for the three studied experiment systems (respiring cells, cell suspensions and crude protein extracts) during dechlorination of TCM by the *Dehalobacter* sp. strain 8M-containing culture. Dotted lines indicate 95% confidence intervals. The error bars represented the uncertainty calculated by error propagation including uncertainties in concentration and isotope measurements.

As mentioned above, respiring cells displayed a slope of $\Lambda^{C/Cl} = 2.8 \pm 0.5$, for the cell suspensions and crude protein extracts experiments the dual element isotope plot showed a slope of $\Lambda^{C/Cl} = 2.5 \pm 0.3$ and $\Lambda^{C/Cl} = 2.7 \pm 0.5$ respectively (Fig. 3C). Consistently, there were not significant differences among the slopes for the three systems ($p > 0.05$). Thus, the slope obtained after integrating the three data sets in one linear regression was $\Lambda^{C/Cl} = 2.8 \pm 0.3$ ($R^2 = 0.94$) (Fig. 3C).

4. Discussion

In this study, we enriched a *Dehalobacter*-containing culture capable of dechlorinating TCM, 1,1,2-TCA, 1,1,1-TCA, 1,1-DCA and TBM. The resulting culture was composed of the genera *Dehalobacter* (20%), *Desulfovibrio* (20%), and *Proteiniphilum* (57%). Species of the genus *Desulfovibrio* have been frequently detected accompanying organohalide-respiring bacteria, including *Dehalobacter* co-cultures that transform TCM (Waite et al., 2020). Previous studies showed that growth of *Desulfovibrio* populations displayed no correlation with TCM dechlorination (Zhao et al., 2017) and that interspecies interactions involving the presence of members of *Desulfovibrio* may benefit the degrading microbial community by mediating acetate and H_2 sources for dechlorinating bacteria (Trueba-Santiso et al., 2020; Wang et al., 2019). Members of *Proteiniphilum* are obligate anaerobic

bacteria that have been shown to metabolize sugars and are expected to degrade oligopeptides, but their role in organohalide-contaminated systems is unclear (Tomazetto et al., 2018). It is hypothesized that they may feed on proteinacious material from dead cells and/or yeast extract in the cultures (Zhao et al., 2017; Tomazetto et al., 2018).

Our results provided evidence that *Dehalobacter* sp. strain 8M gained energy for growth using TCM and 1,1,2-TCA as electron acceptors and is likely the responsible for the transformation of other halogenated compounds as 1,1,1-TCA, 1,1-DCA and TBM. To date, three strains belonging to *Dehalobacter* (strains CF, THM1 and UNSWDHB) and *Desulfitobacterium* sp. strain PR are described to respire TCM (Ding et al., 2014; Grostern et al., 2010; Zhao et al., 2017; Wong et al., 2016). All these strains transform TCM to DCM, except *Desulfitobacterium* sp. strain PR that also produces trace amounts of chloromethane (Ding et al., 2014). The 16S rRNA gene sequence of the strain enriched here, named "*Dehalobacter* sp. strain 8M", shared 99.66% similarity with the 16S rRNA gene of *Dehalobacter restrictus* strain PER-K23. The similarity with *Dehalobacter* strain CF, strain THM1, strain UNSWDHB is 99.21%, 96.81%, and 99.16%, respectively, which indicates that the *Dehalobacter* strain in our culture likely belongs to the species *D. restrictus*. Phylogenetic analysis of the 16S rRNA genes suggests that *Dehalobacter* sp. strain 8M is grouped into a cluster with *D. restrictus* strain PER-K23, strain E1 and strain TeCB1, of which, none of them are known to respire TCM. *D. restrictus* strain PER-K23 is able to use PCE and TCE as electron acceptor and produce *cis*-1,2-dichloroethene (Holliger et al., 1998), strain E1 grows by dechlorination of β-hexachlorocyclohexane to benzene and chlorobenzene (van Doesburg et al., 2005), and strain TeCB1 grows by dechlorination of 1,2,4,5-tetrachlorobenzene and 1,2,4-trichlorobenzene (Alfán-Guzmán et al., 2017). Although strain 8M and strain UNSWDHB share the ability to transform TCM, 1,1,2-TCA and, at a slower rate, 1,1,1-TCA, these two strains differ distinctively in the ratio of vinyl chloride to 1,2-DCA produced from 1,1,2-TCA dechlorination, consisting in 1:1.7 for strain UNSWDHB (Wong et al., 2016) and 1:2.3 for strain 8M. The strong activity of *Dehalobacter* strain CF, strain THM1 and *Desulfitobacterium* sp. strain PR toward 1,1,1-TCA, which is transformed by the TCM-reductive dehalogenases CfrA, ThmA and CtrA, respectively, contrasts with the incomplete and slow degradation of 1,1,1-TCA by *Dehalobacter* strains UNSWDHB (Ding et al., 2014; Zhao et al., 2017; Wong et al., 2016; Tang and Edwards, 2013) and 8M. This finding provides additional supporting evidence that substrate specificity of reductive dehalogenases is not necessarily correlated with the structural similarity of the electron acceptor or the phylogenetic affiliation of organisms. The inefficient degradation of 1,1,1-TCA, 1,1-DCA and TBM might point to a cometabolic degradation of these substrates.

Carbon and chlorine isotope effects were analyzed to pinpoint the reaction mechanism of TCM dechlorination in *Dehalobacter* sp. strain 8M in the light of a recent study that addressed this question with two other *Dehalobacter* strains (strain CF and UNSWDHB) (Heckel et al., 2019). Interestingly, the results indicate that all three *Dehalobacter* strains exhibit distinctive carbon and chlorine isotope fractionation patterns (Table S1). In both strains UNSWDHB and 8M, a small and indistinguishable ($p > 0.05$) carbon isotope effect is observed for TCM dechlorination in respiring cells experiments ($\varepsilon_C = -3.1 \pm 0.5$‰ and -2.8 ± 0.2‰, respectively), whereas degradation by strain CF resulted in a much more pronounced carbon isotope fractionation ($\varepsilon_C = -28 \pm 2$‰). Resulting ε_{Cl} values are significantly different ($p < 0.001$) among these three strains, with a normal chlorine isotope effect for strains CF and 8M ($\varepsilon_{Cl} = -4.2 \pm 0.2$‰ and -0.9 ± 0.2‰, respectively), versus the unexpected inverse chlorine isotope effect observed previously for strain UNSWDHB ($\varepsilon_{Cl} = +2.5 \pm 0.3$‰). For strains UNSWDHB and 8M, however, the carbon and chlorine kinetic isotope effect of the CCl bond cleavage is masked (Table S1). Experiments with cell suspensions and crude protein extracts in strain UNSWDHB resulted in the same small carbon isotopic fractionation as with respiring cells, whereas the inverse chlorine isotope effect increased with the increasing complexity of the system (respiring cells > cell suspensions > crude protein extracts), leading to significantly different 2D-isotope slopes (Heckel et al., 2019). This observation suggested to the authors that contribution

to the inverse chlorine isotope effect was probably due to rate-limiting steps during transport prior to CCl bond cleavage. However, the membrane-associated and periplasm-oriented location of the corresponding TCM reductive dehalogenase is expected to be the same in all Gram-negative *Dehalobacter* (Jugder et al., 2017), including our strain 8M. The authors discarded the nondirected intermolecular interactions and therefore other uncharacterized interactions of TCM with cellular structures were adduced to contribute to the unprecedented inverse isotope effects (Heckel et al., 2019). In our case, however, the similar decrease of the carbon and chlorine isotope effect with higher complexity of the system of strain 8M, resulting in identical $\Lambda^{C/Cl}$ values for the three systems ($p > 0.05$) overruled membrane-induced masking effects. This result is important as it is different from other gram-negative bacteria degrading PCE (Renpenning et al., 2015) or atrazine (Ehrl et al., 2018) where mass transfer through the cell envelope was identified as a relevant rate-limiting step causing masking effects. However, taking into account that AKIEs of crude protein extracts of 8M (without this barrier) were unable to unmask the intrinsic KIE, partially rate-limiting enzyme binding previous to the CCl cleavage can be deduced.

The dual element isotope approach illustrates thus remarkable different ($p < 0.0001$) slopes ($\Lambda^{C/Cl}$) within the strains that have been previously reported to respire TCM (strains CF and UNSWDHB) compared to *Dehalobacter* sp. strain 8M (Table S1 and Fig. 4). In Fig. 4, in addition, characteristic slopes of other TCM degradation processes are presented based on carbon and chlorine isotope fractionation that are also mentioned in Table S1.

In the case of strain CF, the $\Lambda^{C/Cl}$ value (6.6 ± 0.1) was undistinguishable to that obtained for abiotic TCM dechlorination by vitamin B_{12} (6.5 ± 0.2) (Heckel et al., 2019). This was in accordance with an expected common reaction mechanism (likely either outer-sphere-single-electron transfer (OS-SET) or SN2 nucleophilic substitution mechanism) for TCM dechlorination between the reductive dehalogenase of *Dehalobacter* and the cobamide cofactor located within this enzyme (Heckel et al., 2019). A similar $\Lambda^{C/Cl}$ value (7 ± 1) was also obtained from biotic field-derived anoxic microcosms (from a different contaminated site close to Barcelona, Spain) amended with vitamin B_{12} as catalyzer. In that case, pure abiotic reaction with B_{12} was discarded in killed controls (Rodríguez-Fernández et al., 2018b), but biodegradation of TCM did not take place in the live microcosms without this vitamin,

confirming its catalyzing effect. However, active microbial community through 16S rRNA MiSeq high-throughput sequencing revealed that up to now well-known TCM degraders, *Dehalobacter* and *Desulfitobacterium*, were below 0.1% of relative abundance and the *cfr*A gene was not detected. The distinct value of $\Lambda^{C/Cl}$ obtained in the present study for strain 8M ($\Lambda^{C/Cl} = 2.8 \pm 0.3$) compared to the value obtained in the abovementioned contaminated site, may indicate that an important contribution of a *Dehalobacter* sp. strain similar to 8M in that field site is very unlikely.

Further identification and localization of the TCM reductive dehalogenase in *Dehalobacter* sp. strain 8M and its amino acid similarity with TmrA (TCM reductive dehalogenase in strain UNSWDHB) and CfrA (strain CF) will help to understand the distinct isotope fractionation observed in this study and to look for these useful complementary target functional and phylogenetic markers in future field studies.

5. Environmental significance

The widespread presence of TCM in groundwater has led to increased public concern and the need for tools and strategies to achieve its efficient remediation. The present study demonstrates that effective reductive dechlorination of TCM by a novel *Dehalobacter* strain is accompanied by a significant carbon and chlorine isotope fractionation, which can serve as both quantitative and qualitative indicators of anaerobic biodegradation in TCM-impacted groundwaters. But more importantly, dual CCl isotope fractionation pattern during TCM degradation by this novel *Dehalobacter* differs from the fractionation pattern reported for *Dehalobacter* strains CF and UNSWDHB, which would clearly allow to distinguish its contribution to TCM degradation in a field site. In this scenario, when $\Lambda^{C/Cl}$ obtained from site-specific isotopic data coincides with $\Lambda^{C/Cl}$ from reference laboratory experiments, the determined carbon and chlorine isotopic fractionation values are valuable to quantify the degree of in situ biodegradation (%) between the source and a monitoring point (or with time) in the field using the modified Rayleigh equation as recommended by the US EPA guide (Hunkeler et al., 2008). To this regard, taking into account that differences in isotopic compositions in the field for both carbon and chlorine ($\Delta\delta^{13}C$, $\Delta\delta^{37}Cl$) must be >2‰ for being considered significant (Hunkeler et al., 2008), TCM biodegradation from 51% and 89%, respectively would be detectable for strain 8M. In fact, in a previous study in the site from where strain 8M was enriched (Blázquez-Pallí et al., 2019), up to $11 \pm 7\%$ TCM degradation was estimated considering the ε_C reported in literature for *Dehalobacter* sp. strain CF ($\varepsilon_C = -28‰$, (Heckel et al., 2019)). Based on the results of the present work, the extent of biotransformation was very likely underestimated; applying the ε_C calculated here for strain 8M ($-2.8 \pm 0.2‰$) this estimation goes up to $69 \pm 2\%$. This fact emphasizes the importance of using site-specific isotopic fractionation values derived from microcosm experiments prepared with soil and/or groundwater from the contaminated site instead of literature values. Moreover, strain 8M provides a distinct ($p < 0.0001$) $\Lambda^{C/Cl}$ from all the so far described abiotic treatments for TCM remediation (see Fig. 4), which makes this strain a perfect candidate for bioaugmentation treatments because biotransformation of TCM by strain 8M can be distinguished from abiotic transformation and can be reliably quantified by dual-isotopic assessment. The present study data provides key information for practitioners to support the interpretation of stable isotope analyses derived from chloromethanes polluted sites.

Fig. 4. Dual CCl trends during TCM degradation by different strains and different degradation processes (see references in Table S1). Legend: oxidation with persulfate (PS) in red; alkaline hydrolysis (AH) in orange; hydrogenolysis plus reductive elimination by Fe(0) in brown; biodegradation on field-derived anoxic microcosms amended with vitamin B_{12} (Bio B_{12}) in dark green; abiotic dechlorination by vitamin B_{12} (B_{12}) in soft green; outer-sphere single electron transfer (OS-SET) in gray; dehalogenation by *Dehalobacter restrictus* strain CF (strain CF) in black, *D. restrictus* strain UNSWDHB (strain UNSWDHB) in pink, and *Dehalobacter* sp. strain 8M (strain 8M) in blue. Results from cell suspensions and crude protein extract experiments for strains UNSWDHB and 8M are also shown. (For interpretation of the references to colour in this figure legend, the reader is referred to the web version of this article.)

CRediT authorship contribution statement

Jesica M. Soder-Walz: Investigation, Writing – original draft, Formal analysis, Visualization. **Clara Torrentó:** Methodology, Validation, Writing – review & editing. **Camelia Algora:** Methodology, Writing – review & editing. **Kenneth Wasmund:** Methodology, Writing – review & editing. **Pilar Cortés:** Methodology, Validation. **Albert Soler:** Resources. **Teresa Vicent:** Funding acquisition, Project administration, Writing – review & editing. **Mònica Rosell:** Methodology, Validation, Supervision, Writing – review & editing. **Ernest Marco-Urrea:** Supervision, Conceptualization, Writing – review & editing
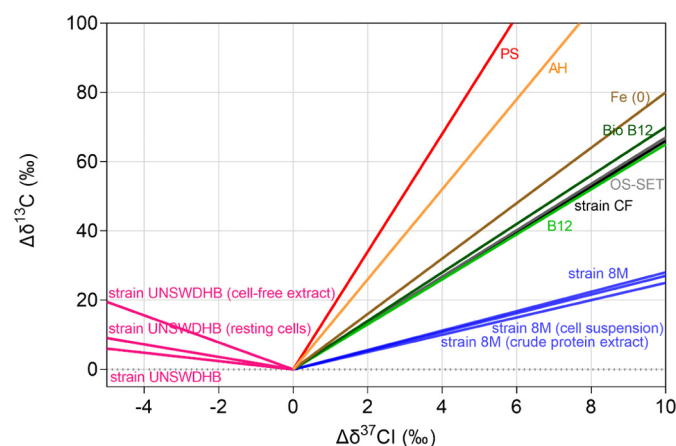
Declaration of Competing Interest

Acknowledgements

Appendix A. Supplementary data

Supplementary data to this article can be found online at https://doi.org/10.1016/j.scitotenv.2021.152659.

References

McCulloch, A., 2003. Chloroform in the environment: occurrence, sources, sinks and effects. Chemosphere 50 (10), 1291–1308. https://doi.org/10.1016/S0045-6535(02)00697-5.

Agency, Environmental Protection, 2000. Chloroform - Hazard Summary. 1 , pp. 1–5.. https://www.epa.gov/sites/production/files/2016-09/documents/chloroform.pdf.

Substance Priority List | ATSDR. (n.d.). Retrieved May 12, 2020, from https://www.atsdr.cdc.gov/spl/#2019spl.

Bagley, D.M., Lalonde, M., Kaseros, V., Stasiuk, K.E., Sleep, B.E., 2000. Acclimation of anaerobic systems to biodegrade tetrachloroethene in the presence of carbon tetrachloride and chloroform. Water Res. 34 (1), 171–178. https://doi.org/10.1016/S0043-1354(99)00121-9.

Cappelletti, M., Frascari, D., Zannoni, D., Fedi, S., 2012. Microbial degradation of chloroform. Appl. Microbiol. Biotechnol. 96 (6), 1395–1409. https://doi.org/10.1007/s00253-012-4494-1.

Jugder, B.E., Ertan, H., Bohl, S., Lee, M., Marquis, C.P., Manefield, M., 2016. Organohalide respiring bacteria and reductive dehalogenases: key tools in organohalide bioremediation. Front. Microbiol. 7 (MAR), 1–12. https://doi.org/10.3389/fmicb.2016.00249.

Ding, C., Zhao, S., He, J., 2014. A Desulfitobacterium sp. strain PR reductively dechlorinates both 1,1,1-trichloroethane and chloroform. Environ. Microbiol. 16 (11), 3387–3397. https://doi.org/10.1111/1462-2920.12387.

Grostern, A., Duhamel, M., Dworatzek, S., Edwards, E.A., 2010. Chloroform respiration to dichloromethane by a dehalobacter population. Environ. Microbiol. 12 (4), 1053–1060. https://doi.org/10.1111/j.1462-2920.2009.02150.x.

Justicia-Leon, S.D., Ritalahti, K.M., Mack, E.E., Löffler, F.E., 2012. Dichloromethane fermentation by a dehalobacter sp. In an enrichment culture derived from pristine river sediment. Appl. Environ. Microbiol. 78 (4), 1288–1291. https://doi.org/10.1128/AEM.07325-11.

Lee, M., Low, A., Zemb, O., Koenig, J., Michaelsen, A., Manefield, M., 2012. Complete chloroform dechlorination by organochlorine respiration and fermentation. Environ. Microbiol. 14 (4), 883–894. https://doi.org/10.1111/j.1462-2920.2011.02656.x.

Kuntze, K., Eisenmann, H., Richnow, H.-H., Fischer, A., 2020. Compound-specific stable isotope analysis (CSIA) for evaluating degradation of organic pollutants: an overview of field case studies. Anaerobic Utilization of Hydrocarbons, Oils, and Lipids. Springer International Publishing, pp. 323–360 https://doi.org/10.1007/978-3-319-50391-2_23.

Nijenhuis, I., Stollberg, R., Lechner, U., 2018. Anaerobic microbial dehalogenation and its key players in the contaminated Bitterfeld-Wolfen megasite. FEMS Microbiol. Ecol. 94 (4). https://doi.org/10.1093/femsec/fiy012.

Vogt, C., Musat, F., Richnow, H.-H., 2020. Compound-Specific isotope analysis for studying the biological degradation of hydrocarbons. Anaerobic Utilization of Hydrocarbons, Oils, and Lipids. Springer International Publishing, pp. 285–321 https://doi.org/10.1007/978-3-319-50391-2_18.

Elsner, M., Zwank, L., Hunkeler, D., Schwarzenbach, R.P., 2005. A new concept linking observable stable isotope fractionation to transformation pathways of organic pollutants. Environ. Sci. Technol. 39 (18), 6896–6916. https://doi.org/10.1021/es0504587.

Nijenhuis, I., Renpenning, J., Kümmel, S., Richnow, H.H., Gehre, M., 2016. Recent advances in multi-element compound-specific stable isotope analysis of organohalides: achievements, challenges and prospects for assessing environmental sources and transformation. Trends Environ. Anal. Chem. 11, 1–8. https://doi.org/10.1016/j.teac.2016.04.001.

Ojeda, A.S., Phillips, E., Sherwood Lollar, B., 2020. Multi-element (C, H, cl, Br) stable isotope fractionation as a tool to investigate transformation processes for halogenated hydrocarbons. <span/>Environ. Sci.: Process. Impacts 22 (3), 567–582. https://doi.org/10.1039/c9em00498j.

Nijenhuis, I., Richnow, H.H., 2016. Stable isotope fractionation concepts for characterizing biotransformation of organohalides. Curr. Opin. Biotechnol. 41, 108–113. https://doi.org/10.1016/j.copbio.2016.06.002.

Rosell, M., Gonzalez-Olmos, R., Rohwerder, T., Rusevova, K., Georgi, A., Kopinke, F.D., et al., 2012. Critical evaluation of the 2D-CSIA scheme for distinguishing fuel oxygenate degradation reaction mechanisms. Environ Sci Technol. 46 (9), 4757–4766.

Renpenning, J., Keller, S., Cretnik, S., Shouakar-Stash, O., Elsner, M., Schubert, T., et al., 2014. Combined C and cl isotope effects indicate differences between corrinoids and enzyme (Sulfurospirillum multivorans PceA) in reductive dehalogenation of tetrachloroethene, but not trichloroethene. Environ Sci Technol. 48 (20), 11837–11845.

Gafni, A., Gelman, F., Ronen, Z., Bernstein, A., 2020. Variable carbon and chlorine isotope fractionation in TCE co-metabolic oxidation. Chemosphere 242, 125130. https://doi.org/10.1016/j.chemosphere.2019.125130 Available from:.

Blázquez-Pallí, N., Shouakar-Stash, O., Palau, J., Trueba-Santiso, A., Varias, J., Bosch, M., Soler, A., Vicent, T., Marco-Urrea, E., Rosell, M., 2019. Use of dual element isotope analysis and microcosm studies to determine the origin and potential anaerobic biodegradation of dichloromethane in two multi-contaminated aquifers. Sci. Total Environ. 696, 134066. https://doi.org/10.1016/j.scitotenv.2019.134066.

Rodríguez-Fernández, D., Torrentó, C., Palau, J., Marchesi, M., Soler, A., Hunkeler, D., Domènech, C., Rosell, M., 2018. Unravelling long-term source removal effects and chlorinated methanes natural attenuation processes by C and cl stable isotopic patterns at a complex field site. Sci. Total Environ. 645, 286–296. https://doi.org/10.1016/j.scitotenv.2018.07.130.

Heckel, B., Phillips, E., Edwards, E., Sherwood Lollar, B., Elsner, M., Manefield, M.J., Lee, M., 2019. Reductive dehalogenation of trichloromethane by two different dehalobacter restrictus strains reveal opposing dual element isotope effects. Environ. Sci. Technol. 53 (5), 2332–2343. https://doi.org/10.1021/acs.est.8b03717.

Heckel, B., Cretnik, S., Kliegman, S., Shouakar-Stash, O., McNeill, K., Elsner, M., 2017. Reductive outer-sphere single electron transfer is an exception rather than the rule in natural and engineered chlorinated ethene dehalogenation. Environ. Sci. Technol. 51 (17), 9663–9673. https://doi.org/10.1021/acs.est.7b01447.

Tschech, A., Pfennig, N., 1984. Growth yield increase linked to caffeate reduction in acetobacterium woodii. Arch. Microbiol. 137 (2), 163–167. https://doi.org/10.1007/BF00414460.

Trueba-Santiso, A., Parladé, E., Rosell, M., Lliros, M., Mortan, S.H., Martínez-Alonso, M., Gaju, N., Martín-González, L., Vicent, T., Marco-Urrea, E., 2017. Molecular and carbon isotopic characterization of an anaerobic stable enrichment culture containing Dehalobacterium sp. During dichloromethane fermentation. Sci. Total Environ. 581–582, 640–648. https://doi.org/10.1016/j.scitotenv.2016.12.174.

Torrentó, C., Palau, J., Rodríguez-Fernández, D., Heckel, B., Meyer, A., Domènech, C., Rosell, M., Soler, A., Elsner, M., Hunkeler, D., 2017. Carbon and chlorine isotope fractionation patterns associated with different engineered chloroform transformation reactions. Environ. Sci. Technol. 51 (11), 6174–6184. https://doi.org/10.1021/acs.est.7b00679.

Hunkeler, D., Aravena, R., Butler, B.J., 1999. Monitoring microbial dechlorination of tetrachloroethene (PCE) in groundwater using compound-specific stable carbon isotope ratios: microcosm and field studies. Environ. Sci. Technol. 33 (16), 2733–2738. https://doi.org/10.1021/es981282u.

Aeppli, C., Hofstetter, T.B., Amaral, H.I.F., Kipfer, R., Schwarzenbach, R.P., Berg, M., 2010. Quantifying in situ transformation rates of chlorinated ethenes by combining compound-specific stable isotope analysis, groundwater dating, and carbon isotope mass balances. Environ. Sci. Technol. 44 (10), 3705–3711. https://doi.org/10.1021/es903895b.

Ojeda, A.S., Phillips, E., Mancini, S.A., Lollar, B.S., 2019. Sources of uncertainty in biotransformation mechanistic interpretations and remediation studies using CSIA. Anal. Chem. 91 (14), 9147–9153.

Chen, G., Kleindienst, S., Griffiths, D.R., Mack, E.E., Seger, E.S., Löffler, F.E., 2017. Mutualistic interaction between dichloromethane and chloromethane degrading bacteria in an anaerobic mixed culture. Environ. Microbiol. 19 (11), 4784–4796. https://doi.org/10.1111/1462-2920.13945.

Kruse, T., Maillard, J., Goodwin, L., Woyke, T., Teshima, H., Bruce, D., et al., 2013. Complete genome sequence of dehalobacter restrictus PER-K23T. Stand. Genomic Sci. 8 (3), 375–388.

Waite, D.W., Chuvochina, M., Pelikan, C., Parks, D.H., Yilmaz, P., Wagner, M., Loy, A., Naganuma, T., Nakai, R., Whitman, W.B., Hahn, M.W., Kuever, J., Hugenholtz, P., 2020. Proposal to reclassify the proteobacterial classes deltaproteobacteria and oligoflexia, and the phylum thermodesulfobacteria into four phyla reflecting major functional capabilities. Int. J. Syst. Evol. Microbiol. 70 (11), 5972–6016. https://doi.org/10.1099/ijsem.0.004213.

Zhao, S., Rogers, M.J., He, J., 2017. Microbial reductive dehalogenation of trihalomethanes by a dehalobacter-containing co-culture. Appl. Microbiol. Biotechnol. 101 (13), 5481–5492. https://doi.org/10.1007/s00253-017-8236-2.

Trueba-Santiso, A., Fernández-Verdejo, D., Marco-Rius, I., Soder-Walz, J.M., Casabella, O., Vicent, T., Marco-Urrea, E., 2020. Interspecies interaction and effect of co-contaminants in an anaerobic dichloromethane-degrading culture. Chemosphere 240. https://doi.org/10.1016/j.chemosphere.2019.124877.

Wang, S., Chen, C., Zhao, S., He, J., 2019. Microbial synergistic interactions for reductive dechlorination of polychlorinated biphenyls. Sci. Total Environ. 666, 368–376. https://doi.org/10.1016/j.scitotenv.2019.02.283.

Tomazetto, G., Hahnke, S., Wibberg, D., Pühler, A., Klocke, M., Schlüter, A., 2018. Proteiniphilum saccharofermentans str. M3/6T isolated from a laboratory biogas reactor is versatile in polysaccharide and oligopeptide utilization as deduced from genome-based metabolic reconstructions. Biotechnol. Rep. 18, e00254. https://doi.org/10.1016/j.btre.2018.e00254.

Wong, Yie K., Holland, S.I., Ertan, H., Manefield, M., Lee, M., 2016. Isolation and characterization of dehalobacter sp. Strain UNSWDHB capable of chloroform and chlorinated

ethane respiration. Environ. Microbiol. 18 (9), 3092–3105. https://doi.org/10.1111/1462-2920.13287.

Holliger, C., Hahn, D., Harmsen, H., Ludwig, W., Schumacher, W., Tindall, B., Vazquez, F., Weiss, N., Zehnder, A.J.B., 1998. Dehalobacter restrictus gen. Nov. And sp. Nov., a strictly anaerobic bacterium that reductively dechlorinates tetra- and trichloroethene in an anaerobic respiration. Arch. Microbiol. 169 (4), 313–321. https://doi.org/10.1007/s002030050577.

van Doesburg, W., Van Eekert, M.H.A., Middeldorp, P.J.M., Balk, M., Schraa, G., Stams, A.J.M., 2005. Reductive dechlorination of β-hexachlorocyclohexane (β-HCH) by a dehalobacter species in coculture with a Sedimentibacter sp. FEMS Microbiol. Ecol. 54 (1), 87–95. https://doi.org/10.1016/j.femsec.2005.03.003.

Alfán-Guzmán, R., Ertan, H., Manefield, M., Lee, M., 2017. Isolation and characterization of dehalobacter sp. Strain TeCB1 including identification of TcbA: a novel tetra- and trichlorobenzene reductive dehalogenase. Front. Microbiol. 8 (APR), 1–13. https://doi.org/10.3389/fmicb.2017.00558.

Tang, S., Edwards, E.A., 2013. Identification of dehalobacter reductive dehalogenases that catalyse dechlorination of chloroform, 1,1,1- trichloroethane and 1,1-dichloroethane. Philos. Trans. R. Soc. Lond., B, Biol. Sci. 368 (1616). https://doi.org/10.1098/rstb.2012.0318.

Jugder, B.E., Bohl, S., Lebhar, H., Healey, R.D., Manefield, M., Marquis, C.P., Lee, M., 2017. A bacterial chloroform reductive dehalogenase: purification and biochemical characterization. Microb. Biotechnol. 10 (6), 1640–1648. https://doi.org/10.1111/1751-7915.12745.

Renpenning, J., Rapp, I., Nijenhuis, I., 2015. Substrate hydrophobicity and cell composition influence the extent of rate limitation and masking of isotope fractionation during microbial reductive dehalogenation of chlorinated ethenes. Environ. Sci. Technol. 49 (7), 4293–4301. https://doi.org/10.1021/es506108j.

Ehrl, B.N., Gharasoo, M., Elsner, M., 2018. Isotope fractionation pinpoints membrane permeability as a barrier to atrazine biodegradation in gram-negative polaromonas spNea-C. Environmental Science and Technology 52 (7), 4137–4144. https://doi.org/10.1021/acs.est.7b06599.

Rodríguez-Fernández, D., Torrentó, C., Guivernau, M., Viñas, M., Hunkeler, D., Soler, A., Domènech, C., Rosell, M., 2018. Vitamin B12 effects on chlorinated methanes-degrading microcosms: dual isotope and metabolically active microbial populations assessment. Sci. Total Environ. 621, 1615–1625. https://doi.org/10.1016/j.scitotenv.2017.10.067.

Hunkeler, D., Meckenstock, R.U., Lollar, B.S., Schmidt, T.C., Wilson, J.T., 2008. A Guide for Assessing Biodegradation and Source Identification of Organic Ground Water Contaminants Using Compound Specific Isotope Analysis (CSIA). U.S. Environmental Protection Agency, Washington, D.C. EPA/600/R-08/148.